

# A study of the proton spectra following the capture of $K^-$ in ${}^6\text{Li}$ and ${}^{12}\text{C}$ with FINUDA

FINUDA Collaboration

M. Agnello<sup>a</sup>, G. Beer<sup>b</sup>, L. Benussi<sup>c</sup>, M. Bertani<sup>c</sup>, H.C. Bhang<sup>d</sup>,  
 S. Bianco<sup>c</sup>, G. Bonomi<sup>e</sup>, E. Botta<sup>f</sup>, M. Bregant<sup>g</sup>, T. Bressani<sup>f</sup>,  
 S. Bufalino<sup>f</sup>, L. Busso<sup>h</sup>, D. Calvo<sup>i</sup>, P. Camerini<sup>g</sup>, P. Cerello<sup>i</sup>,  
 B. Dalena<sup>j</sup>, F. De Mori<sup>f</sup>, G. D'Erasmus<sup>j</sup>, D. Di Santo<sup>j</sup>,  
 D. Elia<sup>k</sup>, F. L. Fabbri<sup>c</sup>, D. Faso<sup>h</sup>, A. Feliciello<sup>i</sup>, A. Filippi<sup>i,1</sup>,  
 V. Filippini<sup>1,2</sup>, R.A. Fini<sup>k</sup>, E. M. Fiore<sup>j</sup>, H. Fujioka<sup>m</sup>,  
 P. Gianotti<sup>c</sup>, N. Grion<sup>n</sup>, O. Hartmann<sup>c</sup>, A. Krasnoperov<sup>o</sup>,  
 V. Lenti<sup>k</sup>, V. Lucherini<sup>c</sup>, V. Manzari<sup>k</sup>, S. Marcello<sup>f</sup>,  
 T. Maruta<sup>p</sup>, N. Mirfakhrai<sup>q</sup>, O. Morra<sup>r</sup>, T. Nagae<sup>p</sup>, A. Olin<sup>s</sup>,  
 H. Outa<sup>t</sup>, E. Pace<sup>c</sup>, M. Pallotta<sup>c</sup>, M. Palomba<sup>j</sup>, A. Pantaleo<sup>k</sup>,  
 A. Panzarasa<sup>1</sup>, V. Patricchio<sup>k</sup>, S. Piano<sup>g</sup>, F. Pompili<sup>c</sup>, R. Rui<sup>g</sup>,  
 G. Simonetti<sup>j</sup>, H. So<sup>d</sup>, V. Tereshchenko<sup>o</sup>, S. Tomassini<sup>c</sup>,  
 A. Toyoda<sup>p</sup>, R. Wheadon<sup>i</sup>, A. Zenoni<sup>e</sup>

<sup>a</sup>*Dip. di Fisica Politecnico di Torino, via Duca degli Abruzzi Torino, Italy, and INFN Sez. di Torino, via P. Giuria 1 Torino, Italy*

<sup>b</sup>*University of Victoria, Finnerty Rd., Victoria, Canada*

<sup>c</sup>*Laboratori Nazionali di Frascati dell'INFN, via E. Fermi 40 Frascati, Italy*

<sup>d</sup>*Dep. of Physics, Seoul National Univ., 151-742 Seoul, South Korea*

<sup>e</sup>*Dip. di Meccanica, Università di Brescia, via Valotti 9 Brescia, Italy and INFN Sez. di Pavia, via Bassi 6 Pavia, Italy*

<sup>f</sup>*Dipartimento di Fisica Sperimentale, Università di Torino, via P. Giuria 1 Torino, Italy, and INFN Sez. di Torino, via P. Giuria 1 Torino, Italy*

<sup>g</sup>*Dip. di Fisica Univ. di Trieste, via Valerio 2 Trieste, Italy and INFN, Sez. di Trieste, via Valerio 2 Trieste, Italy*

<sup>h</sup>*Dipartimento di Fisica Generale, Università di Torino, via P. Giuria 1 Torino, Italy, and INFN Sez. di Torino, via P. Giuria 1 Torino, Italy*

<sup>i</sup>*INFN Sez. di Torino, via P. Giuria 1 Torino, Italy*

<sup>j</sup>*Dip. InterAteneo di Fisica, via Amendola 173 Bari, Italy and INFN Sez. di Bari, via Amendola 173 Bari, Italy*

<sup>k</sup>*INFN Sez. di Bari, via Amendola 173 Bari, Italy*

<sup>1</sup>*INFN Sez. di Pavia, via Bassi 6 Pavia, Italy*

<sup>m</sup>*Dep. of Physics Univ. of Tokyo, Bunkyo Tokyo 113-0033, Japan*

<sup>n</sup>*INFN, Sez. di Trieste, via Valerio 2 Trieste, Italy*

<sup>o</sup>*JINR, Dubna, Moscow region, Russia*

<sup>p</sup>*High Energy Accelerator Research Organization (KEK), Tsukuba, Ibaraki  
305-0801, Japan*

<sup>q</sup>*Dep of Physics Shahid Beheshti Univ., 19834 Teheran, Iran*

<sup>r</sup>*INAF-IFSI Sez. di Torino, C.so Fiume, Torino, Italy and INFN Sez. di Torino,  
via P. Giuria 1 Torino, Italy*

<sup>s</sup>*TRIUMF, 4004 Wesbrook Mall, Vancouver BC V6T 2A3, Canada*

<sup>t</sup>*RIKEN, Wako, Saitama 351-0198, Japan*

---

## Abstract

Momenta spectra of protons emitted following the capture of  $K^-$  in  ${}^6\text{Li}$  and  ${}^{12}\text{C}$  have been measured with 1% resolution. The  ${}^{12}\text{C}$  spectrum is smooth whereas for  ${}^6\text{Li}$  a well defined peak appears at about 500 MeV/c. The first observation of a structure in this region was identified as a strange tribaryon or, possibly, a  $\bar{K}$ -nuclear state. The peak is correlated with a  $\pi^-$  coming from  $\Sigma^-$  decay in flight, selected by setting momenta larger than 275 MeV/c. The  $\Sigma^-$  could be produced, together with a 500 MeV/c proton, by the capture of a  $K^-$  in a deuteron-cluster substructure of the  ${}^6\text{Li}$  nucleus. The capture rate for such a reaction is  $(1.62 \pm 0.23_{stat} {}^{+0.71}_{-0.44}(sys))\%/K^-_{stop}$ , in agreement with the existing observations on  ${}^4\text{He}$  targets and with the hypothesis that the  ${}^6\text{Li}$  nucleus can be interpreted as a  $(d + \alpha)$  cluster.

*PACS:* 21.80.+a, 21.45.+v, 21.30.Fe, 25.80.Nv

*Key words:*  $K^-$  induced reaction in nuclei; proton inclusive spectra; deeply bound  $K^-$ -nucleons states; FINUDA Experiment.

---

## 1 Introduction

The capture process of a negative kaon in a nucleus recently raised renewed interest in the search of the so-called deeply bound  $\bar{K}$ -nuclear systems, predicted by Akaishi and Yamazaki [1]. These states consist of few-body strange ( $S=-1$ ) systems composed of nucleons strongly bound to a  $\bar{K}$ . The strength of the  $\bar{K}N$  attractive interaction, in the  $I=0$  configuration, allows for the stability of

<sup>1</sup> corresponding author. e-mail: filippi@to.infn.it; fax: +39.011.6707324.

<sup>2</sup> deceased

the system, as well as for its compactness [2]. The binding energies predicted for these states are rather sizeable, and the  $\overline{K}N^{(I=0)}$  interaction should be so strong (according to the hypothesis of these Authors) that the widths of these aggregates may be very narrow. In fact, the main decay mode of the  $\overline{K}N$  system is  $\Sigma\pi$ . However, if the potential well is deep enough, even the  $\Sigma\pi$  channel can turn out to be energetically forbidden. In this framework, these states are expected to be formed with larger probabilities in lighter nuclei.

A signal with features compatible to these theoretical expectations was recently found for the ( $K^-$ -three nucleon) system by exploiting the missing mass method (KEK-PS E471 Experiment) [3,4], and for the ( $K^-$ -two nucleon) aggregate by studying the invariant mass of the system (FINUDA at LNF) [5].  $K^-$ 's were stopped in both experiments, on a liquid  ${}^4\text{He}$  target in the first case, and on thin solid targets of several nuclear species ( ${}^6\text{Li}$ ,  ${}^7\text{Li}$ ,  ${}^{12}\text{C}$ ) in the second. E471 claimed evidence for the existence of two different deeply bound  $K^-$ -states, dubbed as  $S^0(3115)$  and  $S^+(3140)$ , observed in the inclusive proton and neutron spectra respectively. They correspond to binding energies of about 193 and 169 MeV, are less than 21 MeV wide and both decay in the  $\Sigma NN$  channel. On the other hand, FINUDA observed a structure decaying into a back-to-back  $\Lambda p$  pair at a mass of about 2255 MeV (corresponding to a binding energy  $B_{K^-pp} = 115^{+6}_{-5}(\text{stat})^{+3}_{-4}(\text{sys})$  MeV), with  $\Gamma = 67^{+14}_{-11}(\text{stat})^{+2}_{-3}(\text{sys})$  MeV.

A further hint for the existence of a strange multibaryon, namely  ${}^{15}_{K^-}\text{O}$ , with a  $K^-$  bound with a binding energy of  $\sim 90$  (or 120) MeV was reported by Kishimoto *et al.* [6] by exploiting the ( $K^-$ ,  $n$ ) reaction at 930 MeV/ $c$ , again based on a missing-mass analysis.

Aside from the mentioned model, other theoretical approaches exist. Some of them admit the existence of bound kaon-nuclear states but with shallower binding potentials [7]; therefore the expected widths of these states are too large to allow their experimental observation.

A dynamical approach, that allows the polarization of the nucleus by the strong  $K^-$ -nucleus interaction, was recently proposed by Mareš *et al.* [8]. In their calculations the depth of the  $\overline{K}$ -nucleus potential is density dependent, and the existence of rather narrow (slightly less than 50 MeV wide) deeply bound kaonic states is expected in nuclei heavier than  ${}^{12}\text{C}$ , for a deep binding energy in the range  $B_{\overline{K}} \sim (100 - 200)$  MeV. This approach suggests that, for the much stronger nuclear polarization obtained in Refs. [3,4] for a target as light as  ${}^4\text{He}$ , any  $\overline{K}$ -nucleus deeply bound state would be too broad to allow clear observation.

Another theoretical argument against the existence of deeply bound kaonic states was put forward by Oset *et al.* [9], who criticize the first theoretical

approach simply showing that the observed signals can be easily explained in terms of few body  $K^-$  absorption reactions and their elementary kinematics. The occurrence of  $K^-$  absorption in nuclei with nucleons emission is indeed a well known process which occurs with a capture rate of the order of 10-20%, so the possibility of observing pions and nucleons in the final state of such processes is sizeable, and this simple interpretation seems to be quite realistic.

We must also recall that the experimental observations obtained so far are not in perfect agreement with the Akaishi-Yamazaki model expectations. In fact, E471  $S^0$  and  $S^+$  states have a binding energy much larger than the predictions from the model. Moreover, their isospin is necessarily equal to one, contrary to the expectation of a singlet isospin configuration to preferentially allow for deeply bound states. Even the observation of a  $(K^- pp)$  bound system by FINUDA is not completely consistent with the features required by this model, especially as far as the isospin and the expected width are concerned. Therefore, the quest for the existence of such states is still open and experimental confirmations are eagerly awaited.

In this paper we report the results of a study of the proton spectra (inclusive and semi-inclusive) emitted in the interaction of  $K^-$  at rest with  ${}^6\text{Li}$  and  ${}^{12}\text{C}$  nuclei, to be compared to the results of Ref. [3,4] on  ${}^4\text{He}$ . The same missing mass analysis technique followed by the Authors of Ref. [3,4] has been basically applied in the present case also. First results of this analysis are reported in Ref. [10].

## 2 Experiment, data selection and spectrum shape analysis

The experiment was performed with the magnetic spectrometer FINUDA, dedicated to Hypernuclear Physics and installed at the DAΦNE  $\phi$  factory at Laboratori Nazionali di Frascati of INFN. Details on the structure of the FINUDA spectrometer, on the measured performance as well as on the conditions of the data taking in the 2003-2004 exploratory run can be found in Refs. [11,12,13]. We recall that the detector features momentum resolution from 0.5 to 1.5% fwhm (depending on the mass and momentum of the charged particle), an angular acceptance close to  $2\pi$  sr and good particle identification. The main apparatus features are briefly sketched in the following. From the beam axis outward three parts can be distinguished, as described hereafter.

- *The interaction/target region.* It is located at the center of the apparatus. Here the kaons from the  $\phi$  decay are identified by means of a 12-thin-slab scintillator array, with the resolution  $\sigma \sim 250$  ps. This barrel is surrounded by an octagonal array of Silicon microstrips (ISIM, acronym for Internal Silicon Microstrips) providing a first precise ( $\sigma \sim 30 \mu\text{m}$ ) position measure-

ment for the determination of the interaction point of the  $K^+$ ,  $K^-$  pairs from of the  $\phi$  decay, in the facing target modules. The target array consists of eight slabs facing the microstrip modules and placed a few millimeters from them, thin enough to stop the  $K^-$  as close as possible to the outer surface of the tile. Different solid materials have been chosen as targets in the 2003-2004 data taking ( ${}^6\text{Li}$ ,  ${}^7\text{Li}$ ,  ${}^{12}\text{C}$ ,  ${}^{27}\text{Al}$ ,  ${}^{51}\text{V}$ );

- *The external tracking device.* It consists of four layers of position sensitive detectors, arranged in coaxial geometry and immersed in a Helium atmosphere to minimize multiple scattering, inside a 1.0 T solenoidal magnetic field. Facing the target tiles a further array of ten Silicon microstrip modules is placed, with basically the same features as the internal ones (OSIM, Outer Silicon Microstrips). The next tracking devices are:
  - i) two octagonal arrays of He- $\text{iC}_4\text{H}_{10}$  (70-30) filled low mass drift chambers, featuring a spatial resolution  $\sigma_{\rho\phi} \sim 150 \mu\text{m}$  and  $\sigma_z \sim 1. \text{ cm}$ ;
  - ii) a straw tube detector, at 1.1 m from the beam axis, composed of six layers of longitudinal and stereo tubes providing a spatial resolution  $\sigma_{\rho\phi} \sim 150 \mu\text{m}$  and  $\sigma_z \sim 0.5 \text{ cm}$ ;
- *The external time-of-flight detector.* The outer TOF detector is a barrel of 72 scintillator slabs, 10 cm thick, providing signals for the first level trigger and time of flight measurements, with a time resolution of  $\sigma \sim 350 \text{ ps}$ . It allows also the detection of neutrons with a  $\sim 10\%$  efficiency and an energy resolution of 8 MeV fwhm, for 80 MeV neutrons.

Out of five different nuclear species used for the eight targets, only  ${}^6\text{Li}$  and  ${}^{12}\text{C}$  were considered in the present analysis. Data collected in the 2003-2004 exploratory run were used.

Figure 1a) shows the inclusive proton spectra for  ${}^6\text{Li}$  (two targets) and Fig. 1b) for  ${}^{12}\text{C}$  (three targets), not acceptance corrected. The acceptance correction is effective only in the lower momentum region of both plots, and doesn't affect the shape in the region beyond 400 MeV/c, where it is basically constant. In the lower momentum region it is a monotonic rising function.

The spectra correspond to  $(3307 \pm 2_{stat} \pm 165_{sys}) \times 10^3$  reconstructed  $K^-$  stops in two  ${}^6\text{Li}$  targets, and  $(4831 \pm 2_{stat} \pm 142_{sys}) \times 10^3$  ones in three  ${}^{12}\text{C}$  targets. A systematic error of 5% can be assigned to these numbers due to a wrong  $K^+/K^-$  identification, based only on kinematics and the position information provided by ISIM, and consequently a wrong assignment of their stopping point in the targets.

The events were selected applying the following criteria:

- i) high quality tracks, *i.e.* long tracks crossing the full spectrometer with a hit on each of the four tracking detectors, selected with the strict requirement of a good  $\chi^2$  out of the track fitting procedure;

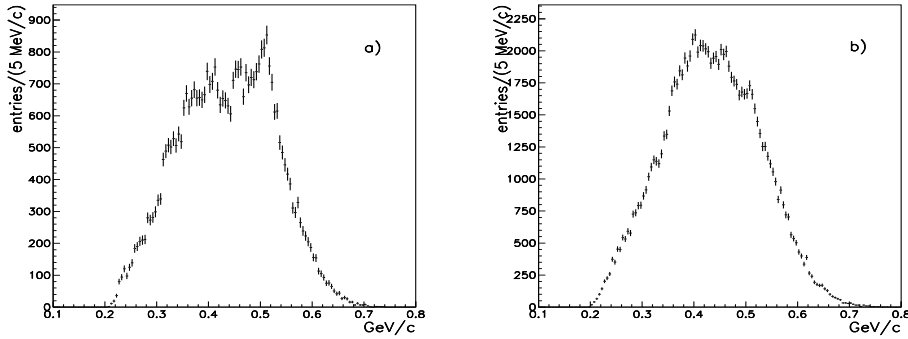


Fig. 1. Inclusive proton spectra measured following the  $K^-$  capture at rest from  ${}^6\text{Li}$  (a) and  ${}^{12}\text{C}$  (b).

- ii) at least one proton per event recognized by particle identification (energy loss in the outer Si-microstrip array) with a probability  $> 94\%$ ;
- iii) a vertex reconstructed inside the fiducial volumes of the chosen targets.

The spectrum for  ${}^{12}\text{C}$  shows a smooth distribution with a maximum around 400 MeV/c and two distortions at about 450 and 520 MeV/c. The distribution is largely due to multinucleon  $K^-$  absorption and, for a fraction, to non-mesonic decays of all kinds of hyperfragments produced following the capture of  $K^-$ . A possible contribution due to protons originating from direct  $(K^-, p)$  reactions in nuclei via weak interactions may be neglected due to the smallness of the expected capture rate. The lower cut at  $\sim 200$  MeV/c is due to the momentum acceptance for four-hit tracks, determined by the size of the spectrometer and the value of the solenoidal magnetic field.

The spectrum of  ${}^6\text{Li}$  shows, in addition to protons from multinucleon  $K^-$  absorption and from non-mesonic decay of the  ${}^5_{\Lambda}\text{He}$ ,  ${}^4_{\Lambda}\text{He}$  and  ${}^4_{\Lambda}\text{H}$  hyperfragments (populating the region between 300 and 450 MeV/c), a prominent and narrow structure peaked at  $\sim 500$  MeV/c.

A feeble signal can also be distinguished at about 580 MeV/c. Probably it is due to the absorption reaction  $K^-(NN) \rightarrow \Lambda N$ , but it's also worth noting that in this region one would expect the emission of deuterons in the rare decay of the hyperhelium fragment  ${}^4_{\Lambda}\text{He} \rightarrow d + d$  (570 MeV/c being the expected momentum value of the emitted deuteron). However, due to the smallness of the expected branching ratio, it is quite unlikely that this reaction could contribute to our inclusive spectrum.

We recall that in Ref. [5] a hint for the existence of a  $(K^-pp)$  bound state decaying into  $\Lambda p$  was put forward. In this case, due to the estimated binding energy of the state (about 110 MeV), the proton momentum should be peaked at  $\sim 420$  MeV/c. The protons from its decay are of course included in Fig 1a) but, given a reported capture rate of the order of  $10^{-3}/(\text{stopped } K^-)$ , one can

safely ignore the contribution of such a channel.

### 3 Data interpretation and discussion

The peak around 500 MeV/ $c$  in the  ${}^6\text{Li}$  spectrum is at about the same position as the inclusive peak observed by E471 in Ref. [3]. Before giving physical interpretations to it, a number of instrumental or elementary physical effects as the possible origin of this signal were studied, and discarded for the reasons discussed in the following.

A first suspect for a possible fake effect comes from the observation that 510 MeV/ $c$  is just the momentum of the ( $e^+$ ,  $e^-$ ) beams stored in the DAΦNE collider to produce the  $\phi(1020)$ , whose decay into ( $K^+$ ,  $K^-$ ) is the source of  $K^-$  for FINUDA. Besides the argument that, if any positron leakage could affect this analysis, one should observe such an effect in both  ${}^6\text{Li}$  and  ${}^{12}\text{C}$  targets, a clear-cut consideration comes from the analysis of the momentum spectrum of negative particles, selected with the same criteria used to recognize the protons. No events were found by requiring negative tracks having the same energy release in the outer array of Si-microstrips as that required for protons. Due to the symmetric behavior of  $e^+$  and  $e^-$ , this possible source of fake events can be safely discarded.

A physical phenomenon which could be a source of 508 MeV/ $c$  protons is the “rare” two-body decay  ${}^4_\Lambda\text{He} \rightarrow {}^3\text{H} + p$ , that should appear in the spectrum from  ${}^6\text{Li}$  but not in  ${}^{12}\text{C}$  since  ${}^4_\Lambda\text{He}$  is one of the few hyperfragments produced from a  ${}^6\text{Li}$  target, but many others may be produced from  ${}^{12}\text{C}$  (the relative production rates account for the different shapes of the spectra in Fig. 1). This proton source was estimated as negligible by the authors of Ref. [3,4] by analyzing the light outputs from the scintillators in order to select “fast” pions accompanying the formation of  ${}^4_\Lambda\text{He}$ . With FINUDA, a very powerful criterion could be adopted exploiting the information provided by the Si-microstrip modules. The energy release of the hits in the ISIM moduli facing the  ${}^6\text{Li}$  targets emitting the proton were asked to be consistent to the passage of a  $\sim 510$  MeV/ $c$   ${}^3\text{H}$  particle.

The number of events fulfilling the condition of a proton in the (480 – 530) MeV/ $c$  range, with a back-to-back particle with an energy release compatible to a triton was ( $58 \pm 8_{stat}$ ). Out of these events, only two have an additional  $\pi^-$  in coincidence. At this stage of the analysis it is rather hard to convert this number into an upper limit for the  ${}^4_\Lambda\text{He} \rightarrow {}^3\text{H} + p$  two-body rare decay due to the uncertainties in the determination of the  ${}^4_\Lambda\text{He}$  production rate. However it is clear that the relative rate of this reaction is negligible and it cannot therefore be the source of an effect as sizeable as the one observed in the data.

To have a better insight into the features of the observed proton peak from  ${}^6\text{Li}$ , a few scatter plots have been studied in order to point out possible correlations between the particles in the peak and other particles of the same event tracked and identified in the apparatus.

The scatter plot of the two momenta for events with two tracks recognized as two distinct protons is reported in Fig. 2a); if the second track is identified as a deuteron, the plot is shown in Fig. 2b).

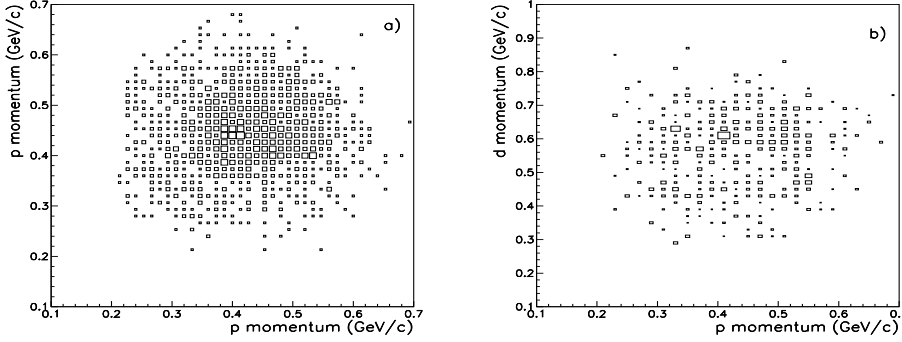


Fig. 2. Two-dimensional scatter plot of the proton momentum versus a) a second proton track or b) a deuteron track, both recognized by specific energy loss, and coming from a common vertex in  ${}^6\text{Li}$  targets.

None of these shows any particular correlation. In Fig. 2a) two enhancements, almost symmetrical in the  $x$  and  $y$  projections, can be seen in the 400 – 450 MeV/ $c$  range with different intensities due to different reconstruction efficiencies for the two tracks. These enhancements can be associated to the  $K^-(pp) \rightarrow \Sigma^0 p$  reaction. In Fig. 2b) the 500 MeV/ $c$  proton signals are correlated to a smooth phase space deuteron distribution, whose lower limit is at about 300 MeV/ $c$  and with a maximum at about 600 MeV/ $c$ .

More interesting is the correlation between the proton spectra of Fig. 1 and the momentum spectra of a  $\pi^-$  emitted from the same vertex. Fig. 3a) shows the scatter plot of the  $\pi^-$  versus proton momentum spectrum for  ${}^6\text{Li}$ , Fig. 3b) for  ${}^{12}\text{C}$ . The main difference between the plots is the presence of a correlation between high-momentum protons ( $\sim 500$  MeV/ $c$ ) with a high-momentum  $\pi^-$  ( $> 300$  MeV/ $c$ ) in  ${}^6\text{Li}$ , that doesn't show up so clearly in  ${}^{12}\text{C}$ .

In figure 4 we report the corresponding  $\pi^-$  momentum spectra for  ${}^6\text{Li}$  and  ${}^{12}\text{C}$ .

Figure 5 shows (white histograms) the proton momentum spectra correlated with a  $\pi^-$ . The grey histograms represent the proton momentum spectra when the coincidence  $\pi^-$  has a momentum larger than, respectively, 275 MeV/ $c$  for  ${}^6\text{Li}$  and 272 MeV/ $c$  for  ${}^{12}\text{C}$  (these values are marked in Fig. 4 with a vertical line). This requirement is due to the fact that  $\pi^-$ 's with momenta lower than

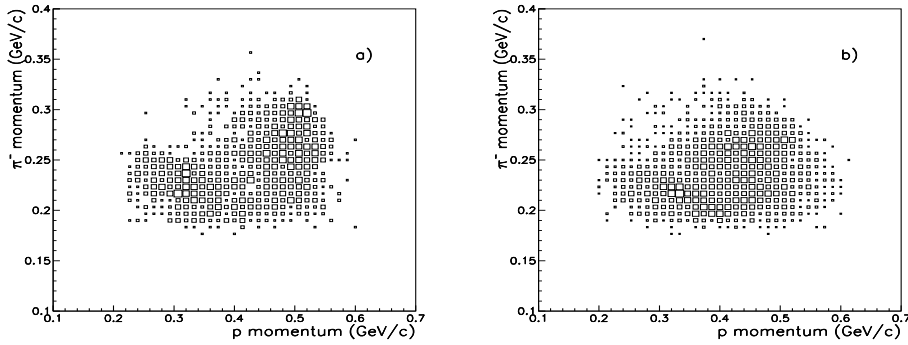


Fig. 3. Two-dimensional plot of the  $\pi^-$  momentum versus the proton momentum from  ${}^6\text{Li}$  (a) and  ${}^{12}\text{C}$  (b).

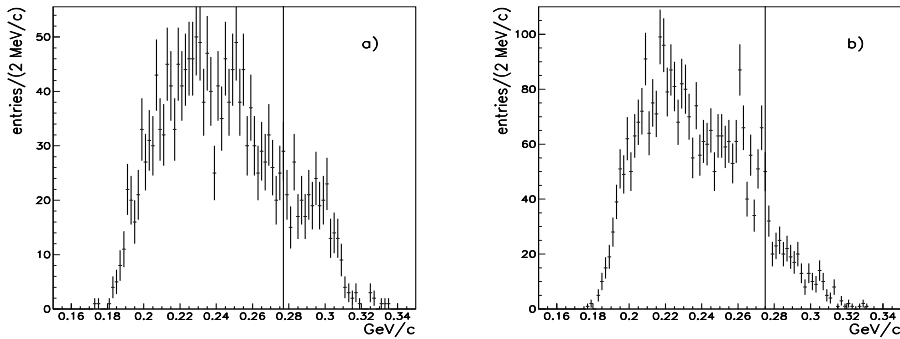


Fig. 4. Momentum spectrum of  $\pi^-$  in coincidence with a proton:  ${}^6\text{Li}$  (a) and  ${}^{12}\text{C}$  (b). The vertical lines indicate the limit for  $\Lambda$  production. The narrow peaks in b) are due to the formation of the ground state and the 10 MeV excited state of  ${}^{\Lambda}_{\Lambda}\text{C}$ .

275 MeV/c for  ${}^6\text{Li}$  and 272 MeV/c for  ${}^{12}\text{C}$  should be mostly associated with the production of  $\Lambda$ -hyperfragments – 275 MeV/c is the kinematical limit for the reaction  $K_{stop}^- + {}^6\text{Li} \rightarrow {}^5_{\Lambda}\text{He} + p + \pi^-$ , while 272 MeV/c is the limit for the reaction  $K_{stop}^- + {}^{12}\text{C} \rightarrow {}^{12}_{\Lambda}\text{C}_{g.s.} + \pi^-$  [12].

A number of  $K^-$  induced reactions on  ${}^6\text{Li}$ , or some substructures of it ( ${}^4\text{He}$ , deuterons), have been studied in order to identify the main source of the observed signature. Indeed, the possibility of interaction of a  $K^-$  on a substructure of a light nucleus like  ${}^6\text{Li}$  is rather sizeable. In fact, in several reactions a  ${}^6\text{Li}$  nucleus was observed to behave like a  $(d + \alpha)$  cluster, with the two nuclei in relative  $s$ -wave. This behavior was in particular observed in  $(\pi^+, 2p)$  reactions in flight [14,15] and  $(\pi^-, 2n)$  reactions at rest [16,17]. The same behavior holds also for  ${}^4\text{He}$ , which can be understood as a cluster of two deuterons. The momentum distribution of a deuteron cluster in  ${}^6\text{Li}$  has two peaks – one at low momentum ( $< 100$  MeV/c), and the other at higher momentum ( $\sim 300$  MeV/c), due to the “quasi”-deuteron contained in the  $\alpha$  cluster (“quasi” here indicates a few-nucleon cluster in a composite nucleus) [18]. On the other

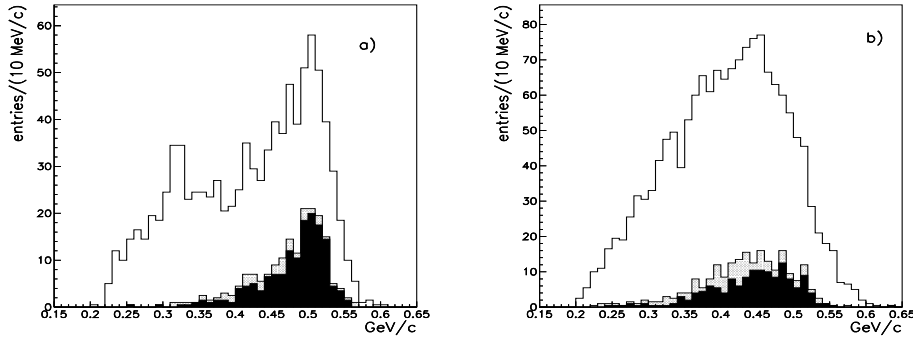


Fig. 5. Momentum spectrum of protons in coincidence with a  $\pi^-$ : a)  ${}^6\text{Li}$ , b)  ${}^{12}\text{C}$ . The shaded spectra are obtained for the condition of a  $\pi^-$  momentum larger than 275 MeV/c for  ${}^6\text{Li}$  and 272 MeV/c for  ${}^{12}\text{C}$ . The black spectra are obtained with the further condition of an angular correlation  $\cos\theta_{(\pi^-p)} < -0.8$ .

hand, for the case of  ${}^4\text{He}$ , the low momentum component is missing and the deuteron momentum distribution has a maximum at about 150 MeV/c.

Therefore, the observed inclusive proton spectra in  ${}^6\text{Li}$  could come from the interaction of a  $K^-$  with a nucleus as a whole, but also with one substructure of it, a “quasi”- ${}^4\text{He}$  or a “quasi”-deuteron. The first case could compare well to the  $K^-$   ${}^4\text{He}$  reaction (as studied from E471). The different distribution of the deuteron momentum in the two cases does not entail large distortions, except a smearing of the signal observed in  ${}^4\text{He}$  as compared to the  ${}^6\text{Li}$  case, so the structures observed in the inclusive spectra out of  ${}^6\text{Li}$  and  ${}^4\text{He}$  could have the same nature. The possibility of disentangling nuclear substructures stands only for light nuclei. In nuclei as heavy as, for instance,  ${}^{12}\text{C}$ , were this reaction still effective, the presence of the surrounding nucleons would severely smear the signal making the observation of such a reaction practically impossible. This fact agrees with the absence of a clean signal in the momentum spectra of protons out of the Carbon targets.

Using the FINUDA data, with the hypothesis that the grey spectrum reported in Fig. 5 is due to the  $K^- + {}^4\text{He} \rightarrow S^0 + p$  reaction, a fit with a Gaussian function of the missing mass spectrum shown in Fig. 6 delivers the values  $m = (3116.4 \pm 3.0)$  MeV and  $\sigma = (25.57 \pm 0.54)$  MeV, respectively, as mass and width of the hypothetical  $S^0$  state (corresponding to a peak momentum value of  $(499.6 \pm 2.2)$  MeV/c). These values were obtained assuming that the signal stands on a background whose shape may be roughly approximated by the shape of the analogous distribution obtained from  ${}^{12}\text{C}$  data that is smoother, not peaked and moved about 40 MeV forward compared to the one from  ${}^6\text{Li}$ . The values obtained are in good agreement with those reported by E471 in Ref. [3]. The contribution from the background amounts to about 30% of the integrated histogram.

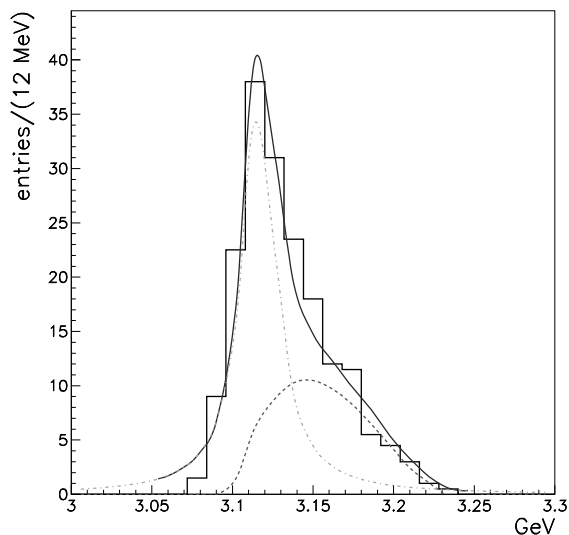


Fig. 6. Missing mass spectrum obtained with the hypothesis of the reaction  $K^- + {}^4\text{He} \rightarrow X + p$ , for data with reconstructed vertices on  ${}^6\text{Li}$  targets; the  ${}^4\text{He}$  nucleus is assumed to be at rest and not subject to any Fermi motion. The dashed curve is a background shape fitting the analogous spectrum obtained for  ${}^{12}\text{C}$  under the same hypothesis, adapted to the tail of the  ${}^6\text{Li}$  distribution; the sum of this contribution to a gaussian fitting the peak, properly weighted, gives the solid line fitting the distribution.

The  $S^0$  is here understood as a  $(K^- pnn)$  bound state; its decay mode is assumed to be the  $YNN$  channel (for a discussion on the possible decay for such states see [2,20]). The measured width is larger than the upper limit of 21 MeV of Ref. [3], in spite of the better momentum resolution. This effect could be easily explained by referring to the internal motion of the “quasi”- ${}^4\text{He}$  cluster inside  ${}^6\text{Li}$ .

The values found for its mass and width were inserted in the simulations of the kinematics of several reactions aiming to single out the one that gives a signature compatible with the observed distributions. In Fig. 7 a summary of the shape of the expected  $\pi^-$  spectra in the following  $K^-$  induced reactions is reported (the branching ratios are not normalized):

- a)  $K^- + d \rightarrow p + \Sigma^-$ , on a deuteron at rest: the expected momentum for the proton is 515 MeV/c, and the  $\Sigma^-$  is forced to decay in flight into  $n + \pi^-$ ;
- b)  $K^- + {}^4\text{He} \rightarrow S^0 + p$ , with the following  $S^0 \rightarrow \Lambda nn$  decay;
- c)  $K^- + {}^4\text{He} \rightarrow S^0 + p$ , with the following  $S^0 \rightarrow \Sigma^- np$  decay;
- d)  $K^- + {}^4\text{He} \rightarrow S^0 + p$ , with the following  $S^0 \rightarrow \Sigma^- np$  decay and  $\Sigma^- p \rightarrow \Lambda n$  conversion;
- e)  $K^- + {}^4\text{He} \rightarrow S^0 + p$ , with the following  $S^0 \rightarrow \Sigma^- d$  decay.

The expected momentum of the proton recoiling against the simulated  $S^0$  is

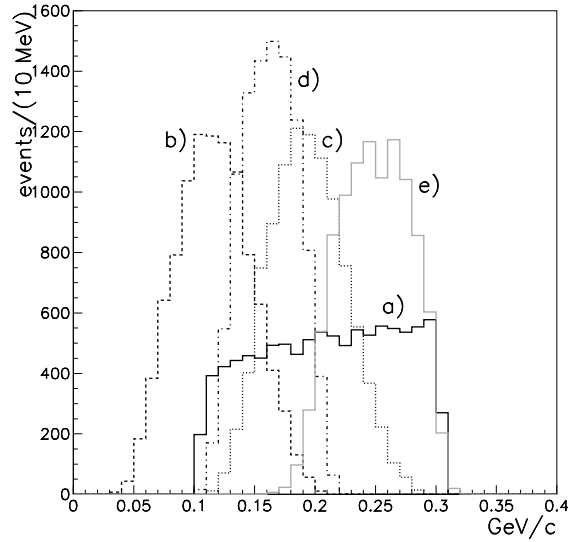


Fig. 7. Monte Carlo momentum spectra for the  $\pi^-$  coming from a hyperon decay together with a  $\sim 500$  MeV/ $c$  proton in the following reactions: a) black solid line:  $K^- + d \rightarrow p + \Sigma^-$ ; b) dashed line:  $K^- + {}^4\text{He} \rightarrow S^0 + p$ , with the following  $S^0 \rightarrow \Lambda nn$  decay; c) dotted line:  $K^- + {}^4\text{He} \rightarrow S^0 + p$ , with the following  $S^0 \rightarrow \Sigma^- np$  decay; d) dotdashed line:  $K^- + {}^4\text{He} \rightarrow S^0 + p$ , with the following  $S^0 \rightarrow \Sigma^- np$  decay and  $\Sigma^- p \rightarrow \Lambda n$  conversion; e) grey solid line:  $K^- + {}^4\text{He} \rightarrow S^0 + p$ , with the following  $S^0 \rightarrow \Sigma^- d$  decay. The spectra show the pure kinematics of the reaction without any filtering through the apparatus acceptance and reconstruction. The hyperon is always assumed to decay in flight. The  ${}^4\text{He}$  and  $d$  target nuclei are assumed to be at rest and not embedded inside a composite nucleus. When they are endowed with a Fermi momentum, which depends on the target nucleus, the distributions are moved toward higher momenta and are more smeared.

501 MeV/ $c$ . The only reactions which could be responsible for the observed signature are a), c) and e) – that means that  $\pi^-$  of momenta larger than the above limits are associated to the in-flight decay of  $\Sigma^- \rightarrow n + \pi^-$  produced either in the quasi two-body reaction  $K^- + (np) \rightarrow \Sigma^- + p$  on correlated  $(np)$  pairs, or deuterons, in the nuclei, or following the decay of the deeply bound  $K^-$ - nuclear states into  $\Sigma^- NN$ . All the nuclei are assumed to be at rest, and no Fermi momentum is assigned in the simulation to any of them.

An experimental confirmation that the  $\pi^-$  comes from a hyperon decay and not exactly from the vertex in which the proton is emitted can be obtained from the study of the impact parameter for the two particles, emitted from the same  ${}^6\text{Li}$  target. The impact parameter is here defined as the distance of closest approach between the  $K^-$  stop point (calculated by tracking the particle inside the target material with GEANE routines [19]) and the particle track, extrapolated backwards to the target region, by means of GEANE routines as well.

Fig. 8 shows the expected distributions after the reconstruction in the FINUDA apparatus of Monte Carlo events with a) an incorrelated pion and proton pair emitted from the same  $K^-$  vertex, and b) a proton and a  $\Sigma^-$  emitted from the  $K^-$  vertex, and a  $\pi^-$  coming from the  $\Sigma^-$  decay.

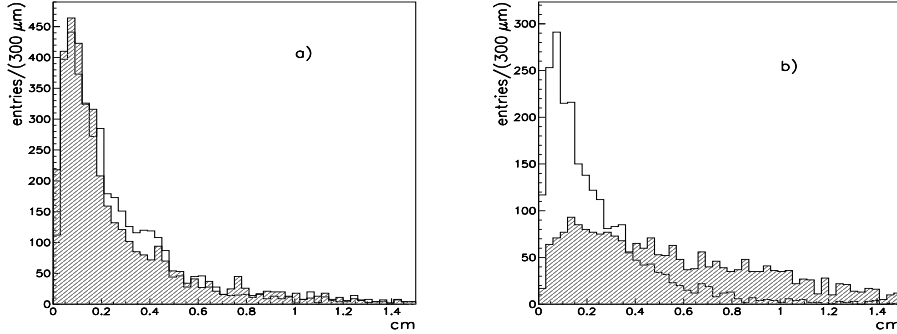


Fig. 8. Distributions of the impact parameter for Monte Carlo data, after reconstruction, in the two cases: a) production of an uncorrelated  $\pi^-$ -p pair from the  $K^-$  vertex, and b) production of  $\Sigma^-$  and  $p$  from the decay vertex, and following  $\Sigma^-$  decay. The open histograms correspond to the proton, and the hatched ones to the  $\pi^-$  case.

While in the first case no difference is seen in the distributions, in the second a substantial shape difference can be appreciated, even if a direct estimation of the decay length cannot easily be deduced. It is noteworthy how in the first case no sensible distortion due to multiple scattering effects affect the two distributions.

The distributions of the distance of closest approach from experimental data are shown in Fig. 9. The shapes of the distributions for the proton (open histogram) and the  $\pi^-$  (hatched histogram) are different and suggest that the pion is most probably produced away from the  $K^-$  vertex, even if the reconstruction algorithm associates the track to the same point.

In the same Figure, the vertical (wavy) hatched histogram shows the experimental distribution for the proton ( $\pi^-$ ) momentum in events where the  $\pi^-$  momentum is required to be larger than 275 MeV/c, corresponding to the shaded histogram in Fig. 5a). In this case, a large difference between the two shapes can be observed, indicating that there is a high probability that the two particles are really emitted from different points.

A handle to understand which of the reactions mentioned above could be the most favorable source for the observed signature is given by the study of the angular correlation (if any) between the  $\pi^-$  and the proton. Were they coming from a reaction like  $d$ ) or  $e$ ), where the proton is emitted together with the deeply bound  $S^0$  state and the  $\pi^-$  comes from the decay of a  $\Sigma^-$  that is one of the products of the decay at rest of the  $S^0$ , no particular angular correlation

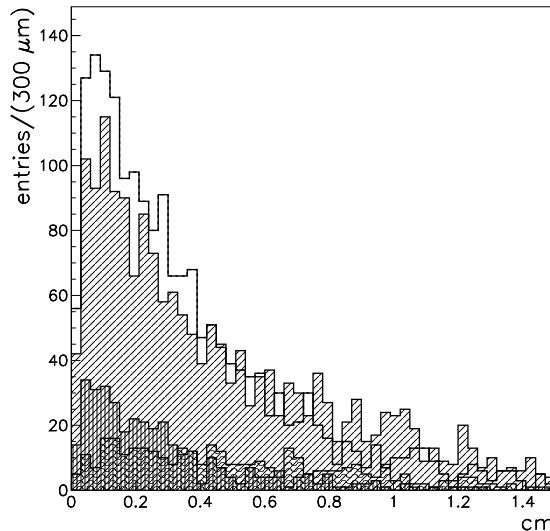


Fig. 9. Distribution of the impact parameter for protons (white histogram) and pions (hatched histogram) following the interaction of a  $K^-$  in the  ${}^6\text{Li}$  targets. The vertical hatched histogram and the wavy one correspond to the proton and  $\pi^-$  impact parameter distributions for events with  $p_{\pi^-} > 275 \text{ MeV}/c$ .

is expected. Even in the case of the formation of a more complicated deeply bound structure in  ${}^6\text{Li}$ , made of five baryons, as could be obtained in the reaction  $K^- + {}^6\text{Li} \rightarrow (K^- ppnnn) + p$ , no angular correlation is expected between the recoiling proton and the  $\pi^-$  presumably coming from the decay of a hyperon among the deeply bound kaonic state decay products.

On the other hand, for a two-body process like *a)* the proton and the  $\Sigma^-$  should be emitted back-to-back, and, if the  $\Sigma^-$  decays in flight, the  $\pi^-$  should keep track of the direction of travel of its mother, therefore an angular correlation should be evident.

Such a correlation was searched for in the coincidence events giving the spectra of Fig. 5a). In Figure 10 the angle between the proton and the  $\pi^-$  track out of the  ${}^6\text{Li}$  targets is shown, properly acceptance corrected. The white histogram corresponds to all the events, while the shaded one to events with a fast  $\pi^-$  ( $p_{\pi^-} > 275 \text{ MeV}/c$ ). The effect of this cut is to eliminate small angle events, keeping mainly back-to-back correlated ones. By requiring the condition  $\cos\theta_{(\pi^-p)} < -0.8$ , the black distributions shown in Fig. 5 were obtained for both  ${}^6\text{Li}$  and  ${}^{12}\text{C}$  targets: the peak in  ${}^6\text{Li}$  data is still prominent and possibly shrinks, while this selection has no particular effect on the distribution out of  ${}^{12}\text{C}$ .

This observation is the most convincing proof in favor of the two-body reaction on two nucleons with  $\Sigma^-p$  production, and against the production of a deeply

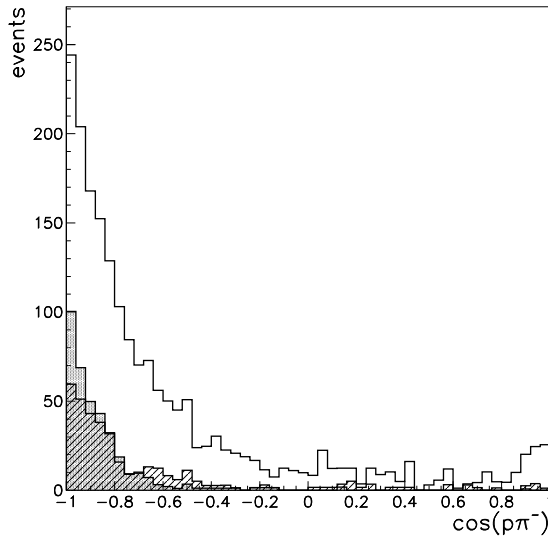


Fig. 10. Distribution of the angle between a proton and a  $\pi^-$  track following the interaction of a  $K^-$  in the  ${}^6\text{Li}$  targets: the white histogram is for all events, the shaded one for events with the pion momentum larger than 275 MeV/c, the hatched one for events with the proton momentum in the window (275 – 350) MeV/c. All the distributions are acceptance corrected and normalized to the number of selected events in each sample.

bound  $K^-$  state with the features suggested by E471. Since the missing mass spectrum analysis pointed out a close familiarity between the signal observed by FINUDA and the one seen by E471, it might be plausible, in this view, that the peak observed in the  $K^-$   ${}^4\text{He}$  reaction could be due to the interaction of the  $K^-$  on a deuteron-like substructure of the E471  ${}^4\text{He}$  target; therefore it appears to be unnecessary to invoke the existence of one or even two deeply bound  $K^-$  states to explain it.

### 3.1 Comments on the spectrum shape at lower momenta ( $\sim 300$ MeV/c).

Figure 5a) shows clearly a further structure at about 300 MeV/c, that can be interpreted as a further hint to a  $(\alpha+d)$  behavior of  ${}^6\text{Li}$  in the  $K^-$  capture. The possibility that it might be due to an acceptance effect can be rather safely discarded since, as such, it should also be visible in the  ${}^{12}\text{C}$  case. Moreover, the acceptance function in this region is steeply rising, but is smooth and doesn't exhibit any structure.

Therefore, we suggest attributing it to the reaction  $K^- + n \rightarrow \Lambda + \pi^-$  occurring on a neutron of the deuteron cluster. The internal momentum of such a neutron in the quasi-deuteron substructure is low, given *e.g.* by the well-known Hulthén formula; the momentum of the quasi-deuteron relative to the  $\alpha$ -cluster is very

small, as previously mentioned [15]. The total momentum of the neutron inside a quasi-deuteron cluster is lower than 100 MeV/c. So the reaction on a neutron in a quasi-deuteron cluster shows basically the same kinematic features of the reaction on a free neutron, with the momenta of both  $\Lambda$  and  $\pi^-$  around 250 MeV/c. The  $\Lambda$  decays in flight in a (forward emitted) proton with a momentum of about 300 MeV/c, and a  $\pi^-$  with a momentum around 110 MeV/c. This pion escapes the momentum acceptance of the reconstruction procedure, and therefore goes undetected. In Fig. 4a) a hint of a peak for  $\pi^-$  around 250 MeV/c can be seen, and the scatter plot of Fig. 3a) also shows a correlation between 300 MeV/c protons and  $\sim 250$  MeV/c  $\pi^-$ .

The distribution of the angle between a proton with momentum selected in the window (275 – 350) MeV/c and the  $\pi^-$  is reported in the hatched histogram in Fig. 10. Even in this case there is a marked preference for a back-to-back topology, consistent with the hypothesis that the proton comes from the  $\Lambda$  decay, with the  $\Lambda$  emitted in the opposite direction to the  $\pi^-$ , in the  $K^- + n \rightarrow \Lambda + \pi^-$  reaction occurring almost at rest.

### 3.2 Evaluation of the capture rate for the $K^- + (np) \rightarrow \Sigma^- + p$ reaction in ${}^6\text{Li}$

The evaluation of the capture rate for negative kaons inducing the two-body reaction under examination is based on their tagging by means of the  $\mu^+$  or  $\pi^+$  from the decay of the  $K^+$  emitted in the  $\phi$  decay. Out of the selected events, the total number of kaons to which the selected sample is normalized is obtained selecting those having also a positive track correctly identified as a  $\mu^+$  or  $\pi^+$ . This track must come from a target opposite to the one where the  $K^-$  stopping occurs.

The capture rate for the selected events in coincidence with a  $\mu^+$  or a  $\pi^+$  from the opposite target (*tagged* events) is given by

$$R = \frac{N_{ev}^{tag}}{N(K_{stop}^{-tag}) \cdot \epsilon_D(ev) \cdot \epsilon_G^{tag}(ev)} \quad (1)$$

where  $N(K_{stop}^{-tag})$  is the number of  $K^-$ 's stopping in the given target (for  $\mu^+/\pi^+$  tagged events),  $\epsilon_D(ev)$  is the detector efficiency for the selected events and  $\epsilon_G(ev)$  is the global efficiency taking into account the trigger and the reconstruction efficiency and the geometrical acceptance of the apparatus. For events with a coincidence  $\mu^+/\pi^+$  the trigger efficiency is practically equal to one, so  $R$  can be considered, in this case, as independent of the trigger efficiency. We recall that the trigger applied (mainly to select hypernuclear formation events) required two back-to-back slabs firing on the internal scin-

tillator barrel, with signal amplitude above an energy threshold accounting for the high ionization of slow kaons, and a fast coincidence on the external scintillator barrel, to account for the presence of a  $\mu^+$  from the  $K^+$  decay.

The global efficiency for the selected events is given, as usual, by

$$\epsilon_G^{tag}(ev) = \frac{N_{ev}^{tag,MC}}{N(K_{stop}^{-tag,MC})}, \quad (2)$$

while the detector efficiency  $\epsilon_D(ev)$  must be carefully evaluated since the typical event is composed of two four-point tracks almost back-to-back. For a four point track fully reconstructed in a selected apparatus region (depending on the target position), the detector efficiency can be deduced by the simulation of well known reactions, such as  $K_{\mu 2}$  decay, comparing the simulated and experimental decay branching ratios obtained for well identified muons emitted from the same target. One can roughly assume that the detector efficiency for the two prongs of a typical event of the reaction under study may be given by the combination of the efficiencies of two single tracks – one emitted in the forward direction, and one in the backward hemisphere with respect to the chosen target. On an event-by-event basis, it would be possible to assign to each single track the correct forward/backward detector efficiency. In the rate calculation, however, this assignment is not possible. So, as a first approximation and on average, the detector efficiency for each track is assumed to be equal to the efficiency for positive muons emitted in both the hemispheres, and crossing almost the whole apparatus. However, the systematic error affecting this approximate procedure in the detector efficiency evaluation does not exceed 0.7% of the evaluated rate.

In Tab. 1 the relevant numbers to get the  $R$  values for the two  ${}^6\text{Li}$  targets are reported.

$N_{ev}^{tag}$	$N(K_{stop,tag}^-)$	$\epsilon_G^{tag}(ev) \times 10^3$	$\epsilon_D(ev)$	$R/K_{stop}^- (\%)$
10±3	347174±589 <sub>stat</sub> ±17359 <sub>sys</sub>	9.0±0.8	0.229±0.008	1.43±0.62 <sub>stat</sub> $^{+0.20}_{-0.07}$ (sys)
23±5	363745±603 <sub>sys</sub> ±18187 <sub>sys</sub>	11.1±0.8	0.313±0.008	1.85±0.56 <sub>stat</sub> $^{+0.30}_{-0.09}$ (sys)

Table 1

Measured number of events,  $K^-$  stops, efficiency and capture rate for the reaction  $K^- + (pn) \rightarrow \Sigma^- p$ . The number of events and of stops are both tagged with a coincidence  $\mu^+$  or  $\pi^+$  on the opposite target. The number of selected events for the reaction under study is already background subtracted (the background amounts to about 30% of the observed signal). The two lines correspond to events collected on two different  ${}^6\text{Li}$  targets.

A second way to determine the capture rate of the studied reaction is based on the normalization on the number of  $\mu^+$ 's produced by  $K^+$ 's stopping in the same target. In this way two particles of the two reactions cross approximately

the same region of the apparatus. The detector efficiencies roughly cancel out for tracks of the same sign (muons and protons), and only the detector efficiency for  $\pi^-$ 's and the global efficiencies of each reaction must be evaluated, again by means of a dedicated simulation of both the reaction under study and of the  $K_{\mu 2}$  decay occurring in the chosen target. Again we assume that, without any selection on the direction, the detector efficiency for  $\pi^-$  is roughly equal to that estimated for muons emitted from the same target. This is due to the fact that almost similar tracks span is the same apparatus region, independently of the particle charge.

The capture rate  $R'$  is therefore evaluated by the formula

$$R' = \frac{N(ev)}{N_{\mu^+}} \cdot \frac{N(K_{stop}^+)}{N(K_{stop}^-)} \cdot \frac{\epsilon_G(\mu^+)}{\epsilon_G(ev)} \cdot \frac{\epsilon_D(\mu^+)}{\epsilon_D(ev)} \quad (3)$$

Tab. 2 reports the relevant numbers to get the  $R'$  values for the two  ${}^6\text{Li}$  targets.

$N(ev)$	$N_{\mu^+}$	$N(K_{stop}^+)$	$N(K_{stop}^-)$
$113 \pm 11_{stat} \pm 11_{sys}$	$76475 \pm 277$	$1214996 \pm 1102_{stat} \pm 60750_{sys}$	$1535943 \pm 1239_{stat} \pm 76797_{sys}$
$132 \pm 11_{stat} \pm 2_{sys}$	$92031 \pm 303$	$1414073 \pm 1189_{stat} \pm 70704_{sys}$	$1771202 \pm 1331_{stat} \pm 88560_{sys}$
$\epsilon_G(\mu^+)$	$\epsilon_G(ev) \times 10^3$	$\epsilon_D(\mu^+)$	$R'/K_{stop}^-(\%)$
$0.129 \pm 0.002$	$14.6 \pm 0.5$	$0.489 \pm 0.011$	$2.22 \pm 0.45_{stat} \begin{smallmatrix} +0.22 \\ -0.25 \end{smallmatrix} (sys)$
$0.126 \pm 0.002$	$15.9 \pm 0.4$	$0.561 \pm 0.011$	$1.50 \pm 0.27_{stat} \begin{smallmatrix} +0.15 \\ -0.17 \end{smallmatrix} (sys)$

Table 2

Measured number of events,  $K^-$  and  $K^+$  stops in the same  ${}^6\text{Li}$  target, and capture rate for the reaction  $K^- + (pn) \rightarrow \Sigma^- p$  evaluated using the method of  $\mu^+$  normalization ( $K_{\mu 2}$  decays from the same target as the reaction under study). The number of selected events is already background subtracted (the background amounts to about 30% of the observed signal). The two lines correspond to events collected on two different  ${}^6\text{Li}$  targets.

The values of  $R$  and  $R'$  for both the targets are in agreement, within the statistical error, except for the value of  $R'$  for the first  ${}^6\text{Li}$  target, which is compatible with the  $R$  measurement from the same target within  $2\sigma$  only. We assume that a total statistical error as big as the largest of the two measurements on the same target can be assigned to their weighted mean value.

Therefore, one gets for the weighted means of the evaluated rates for the two  ${}^6\text{Li}$  targets (denoted in the following as 1 and 2) the two capture rates:  $R_1 = (1.94 \pm 0.62_{stat} \begin{smallmatrix} +0.20 \\ -0.22 \end{smallmatrix} (sys))\% / K_{stop}^-$  and  $R_2 = (1.57 \pm 0.24_{stat} \begin{smallmatrix} +0.18 \\ -0.37 \end{smallmatrix} (sys))\% / K_{stop}^-$ ; their mean value is  $(1.62 \pm 0.23_{stat} \begin{smallmatrix} +0.71 \\ -0.44 \end{smallmatrix} (sys))\% / K_{stop}^-$ , to be compared to previous measurements of the  $K^-$  induced reaction obtained in bubble chamber experiments. Ref. [21] reports a multinucleonic  $K^-$  capture rate at rest of the order of  $\sim 10\%$  in Deuterium,  $\sim 16\%$  in Helium and  $\sim 20\%$  in Carbon: the

absorption rate is assumed to remain rather constant beyond  $A = 4$ , perhaps increasing slowly for heavier nuclei where the absorption most likely occurs on the nuclear surface. Out of all the multinucleonic  $K^-$  capture events in Helium, according to Ref. [22] the rate for  $K^- \text{}^4\text{He} \rightarrow \Sigma^- pd$  is  $(1.6 \pm 0.6)\% / K_{stop}^-$ , while for  $K^- \text{}^4\text{He} \rightarrow \Sigma^- ppn$  is  $(2.0 \pm 0.7)\% / K_{stop}^-$ .

These figures are in fair agreement with the results obtained in the present analysis. They can be directly compared for the case of the  $K^- \text{}^4\text{He}$  reaction where the  $d$  or  $(np)$  in the final state can be assumed as spectators.

## 4 Conclusions

The inclusive proton momentum spectrum in  $K^-$  reactions induced in  ${}^6\text{Li}$  exhibits a sharp structure at about 500 MeV/ $c$  which can be rather easily explained as due to the interaction of the  $K^-$  on a “quasi”-deuteron cluster in the  ${}^6\text{Li}$  nucleus, leading to the two-body final state  $\Sigma^- + p$ . Both the observed proton and the  $\pi^-$  from the  $\Sigma^-$  decay have the right kinematic features to confirm that they belong to this reaction. Moreover, the rate for such a reaction is compatible with the rates of similar reactions observed in helium bubble chamber experiments.

Since the signal is quite similar to the observations of E471 in  $K^-$  induced reactions on a  ${}^4\text{He}$  target, the peaks observed by the two experiments could have the same nature, and maybe they are simply due to a two-body reaction where a  $K^-$  interacts on a “quasi” deuteron, both in  ${}^6\text{Li}$  and in  ${}^4\text{He}$ . This possibility makes the claim for a deeply bound state unnecessary. On the other hand, the absence of such a signal in the spectra out of  ${}^{12}\text{C}$  targets strengthens this hypothesis, as a similar two-body mechanism would be possible even on  ${}^{12}\text{C}$  nuclei, but very difficult to observe because of the size of the whole nuclear system and the dilution effects it entails.

Thus, we point out that the possibility of selective capture by clusters in nuclei can be the source of ambiguities in missing mass experiments. Invariant mass measurements, exclusive and more precise, would probably help to better clarify the interesting subject of the existence of such states, supported by complementary information obtained with the missing mass method. In fact, it must be reminded that the first experimental observation with the invariant mass technique, performed by FINUDA, although more precise, presents a few inconsistencies compared to the expectations of some theoretical models. So, on one side more experimental data are urgently needed, to confirm the observed structures and to check for possible different decay patterns. On the other hand, further theoretical calculations are required to explain the experimental observations and possibly discard their interpretation as  $\overline{K}$ -nuclear

states.

## 5 Acknowledgments

We are indebted to Prof. T. Yamazaki for enlightening discussions and Prof. A. Gal for precious suggestions and remarks. We thank the DAΦNE crews for their skillful handling of the collider and the FINUDA technical staff for their constant support.

## References

- [1] Y. Akaishi and T. Yamazaki, *Phys. Rev.* **C65** (2002), 044005
- [2] A. Doté *et al.*, *Phys. Lett.* **B590** (2004), 51;  
A. Doté *et al.*, *Phys. Rev. C* **70** (2004), 044313
- [3] T. Suzuki *et al.*, *Phys. Lett.* **B597** (2004), 263
- [4] T. Suzuki *et al.*, *Nucl. Phys.* **A754** (2005), 375c
- [5] M. Agnello *et al.*, *Phys. Rev. Lett.* **94** (2005), 212303
- [6] T. Kishimoto *et al.*, *Nucl. Phys.* **A754** (2005), 383c
- [7] J. Schöffner-Bielich *et al.*, *Nucl. Phys.* **A669** (2000), 153;  
A. Ramos and E. Oset, *Nucl. Phys.* **A671** (2000), 481;  
A. Cieply *et al.*, *Nucl. Phys.* **696** (2001), 173
- [8] J. Mareš *et al.*, *Nucl. Phys.* **A770** (2006), 84
- [9] E. Oset and H. Toki, preprint nucl-th/0509048  
V.K. Magas *et al.*, preprint nucl-th/0601013
- [10] A. Filippi *et al.*, FINUDA Collaboration, in *Proceedings of Eleventh International Conference on Hadron Spectroscopy*, Rio de Janeiro, Brazil, 21–26 August 2005, ed. A. Reis *et al.*, AIP Conference Proceedings **814**, Melville, New York (2006), p. 598
- [11] M. Agnello *et al.*, *Nucl. Phys.* **A754** (2005), 399c
- [12] M. Agnello *et al.*, *Phys. Lett.* **B622** (2005), 35
- [13] A. Zenoni in *Proc. Int. School of Physics “E. Fermi” Course CLVIII (Hadron Physics)*, eds T. Bressani, U. Wiedner and A. Filippi, S.I.F. - IOS Press (2005), 183
- [14] T. Bressani *et al.*, *Nucl. Phys.* **B9** (1969), 427

- [15] J. Favier *et al.*, *Nucl. Phys.* **A169** (1971), 540
- [16] C. Cernigoi *et al.*, *Nucl. Phys.* **A352** (1981), 343
- [17] C. Cernigoi *et al.*, *Nucl. Phys.* **A456** (1986), 599
- [18] T. Yamazaki and S. Hirenzaki, *Phys. Lett.* **B557** (2003), 20
- [19] V. Innocente *et al.*, GEANE, Average Tracking and Error Propagation Package, CERN Program Library, W5013-E, 1991
- [20] J. Mareš *et al.*, *Phys. Lett.* **B606** (2005), 295
- [21] C. Vander Velde-Wilcquet *et al.*, *Il Nuovo Cimento* **39A** (1977), 538
- [22] P.A. Katz *et al.*, *Phys. Rev.* **D1** (1970), 1267